Hindawi
International Journal of Antennas and Propagation
Volume 2023, Article ID 4839134, 13 pages
https://doi.org/10.1155/2023/4839134

Research Article

An Isolation Improvement for Closely Spaced MIMO Antenna Using $\lambda/4$ Distance for WLAN Applications

E. Suganya,[1] **T. Prabhu**,[2] **Satheeshkumar Palanisamy**,[3] **Praveen Kumar Malik**,[4] **Naveen Bilandi**,[5] **and Anita Gehlot**[6]

[1]*Department of Electronics and Communication Engineering, NITTE Meenakshi Institute of Technology, Bengaluru, Karnataka, India*
[2]*Department of Electronics and Communication Engineering, Presidency University, Bengaluru, Karnataka, India*
[3]*Department of Electronics and Communication Engineering, Coimbatore Institute of Technology, Coimbatore, India*
[4]*School of Electronics and Electrical Engineering, Lovely Professional University, Jalandhar 144001, Punjab, India*
[5]*DAV University, Jalandhar, Punjab, India*
[6]*Uttaranchal Institute of Technology, Uttaranchal University, Dehradun, Uttarakhand 248007, India*

Correspondence should be addressed to Praveen Kumar Malik; praveen.23314@lpu.co.in

Received 17 September 2022; Revised 16 October 2022; Accepted 21 April 2023; Published 10 May 2023

Academic Editor: Maggie Y. Chen

An isolation improvement for a closely spaced quad port multiple-input multiple-output (MIMO) antenna for WLAN applications is presented. The proposed antenna consists of four L-shaped monopole microstrip patch antennas with a rectangular slot at the center and truncated edges at the corner of each patch element. Interelement isolation is improved by more than 12 dB by considering the patch size, ground size, and distance between the patch elements. The designed antenna uses $\lambda/4$ distance between the patch elements. The slot in each patch improves the bandwidth, and truncated edges at the corner of the patch improve the impedance matching of the antenna. The proposed MIMO antenna is designed with the overall dimensions of 45.5 mm × 45.5 mm × 1.96 mm. The MIMO parameters for the proposed technique, which include envelope correlation coefficient (E.C.C.) are less than 0.5, and the diversity gain (D.G.) is 10 dB, suggesting this antenna's suitability for MIMO operations. The average peak realized gain (A.P.R.G.) and radiation efficiency (RE) is 2.8 dBi and greater than 80% for the prescribed band of interest. The antenna element is fabricated and tested using microwave analyzer N9917A. The measured result seems to be in good contact with the simulation. The proposed MIMO antenna is well-suitable for WLAN applications.

1. Introduction

Current wireless communication depends on the data rate and quality of information transferred. These factors were considered and identified that multiple-input multiple-output technology could satisfy these needs. MIMO technology overcomes specific effects like scattering, fading and multipath transmission, and reception. The researcher is investigating new methodologies to operate multiple antennas due to the ever-increasing demand for superior data rates to cater to which MIMO technology is considered one possible candidate [1], and the physical limitations of wireless devices pose few challenges. Mutual coupling between antennas lowers their efficiency since some of their power is emitted to the nearby antennas.

Furthermore, this coupling may cause them to interfere with one another. As a result, antenna isolation improvement techniques have become a highly required topic. Limiting radiation in the propagation direction and increasing the distance between the antennas are two common ways to improve isolation. However, this strategy is inefficient due to the tiny amount of space provided for antennas in mobile devices. Several studies on spatial diversity and MIMO systems have been conducted to increase isolation performance. With the usage of MIMO technology, not only are the factors reduced but this technology also

increases the capacity of channels without making any modifications to the previous structure of the design.

The antenna designed using this MIMO method depends on applications like Wi-Fi, Wi-Max, WLAN, and I.T.U. Bands for wireless devices [2]. However, the speed of data transmission and channel capacity must be considered. On empathizing, mutual coupling arises when multiple antennas are placed. The coupling effect should be controlled for implementing many antennas in the system. It takes more time to transmit the data with minimum antennas, and an ideal methodology can be used to improve the antenna performance. The abovementioned limitations can be overwhelmed by implementing multiple-input multiple-output (MIMO) antennas [3]. Although the usage of the MIMO antenna accomplishes higher isolation standards and a common correlation effect, two crucial things have to be considered when designing a MIMO antenna [4]. First, the antenna size should be compact for wireless applications [5]. Second, the mutual coupling should be limited to closer radiating elements [6]. In this paper, we proposed a low profile, L-shaped resonator with a rectangular slot at the center, and truncated edges at the individual corner of the patches are used to enhance isolation for interelement antennas and also improve the diversity performances of the MIMO antennas, which includes the MIMO parameters like mean effective gain (M.E.G.), diversity gain (D.G.), and envelope correlation coefficient (E.C.C.).

This paper is systematized as follows. Section II implicates the related works, where the coaxially fed, linearly polarized, low profile, L-shaped resonator with a rectangular slot on the patch is analyzed. Section III discusses the configuration and geometry of the MIMO antenna. Section IV discusses the equivalent electric circuit model of the proposed MIMO antenna. Section V investigates the performance of the MIMO antenna with results and discussions. Finally, in Section VI, the conclusion is discussed.

2. Related Works

The following section explores the various antenna and MIMO parameters considered for designing an efficient antenna structure. Many researchers found different techniques to improve the mutual coupling for closely spaced antenna elements to cancel the self-induced currents by antenna elements. For instance, by introducing the defected ground structure (DGS) [7–9], complementary split ring resonator (CSRR) [10–12], neutralization line (NL) [13–15], frequency reconfigurable (FR) [16–18], electromagnetic band gap (EBG) [19–22], metamaterial (MM) [23–25], decoupling network (DN) [26–28], dielectric resonator antenna (DRA) [29–31], and parasitic strip (PS) [32, 33] and introducing different shapes like inverted L [34], modified T shape [35, 36] F shape [37], and meta surface [38–44] improve mutual coupling and the isolation of more than 20 dB is achieved. However, MIMO antenna parameters like diversity gain (D.G.), envelope correlation coefficient (E.C.C.), and radiation efficiency (RE) need to be considered for improving the channel capacity with any additional power [45].

Since the same isolation mechanism typically does not function across various frequency bands, designing a dual-band, MIMO antenna presents its unique set of challenges. Multiple multi-input multi-output (MIMO) antennas have been previously reported [46]. Adding numerous branches and a shorting pin improves isolation between two adjacent dual-band monopole antennas [47]. In [48], two folded monopoles employed with mutual coupling decreased through transmission lines on the upper surface and slots on the ground plane. The monopole antenna in [49] is of the four-shaped variety. When the defective ground structure is introduced, the isolation increases. In [50], a multi-input multi-output (MIMO) antenna is designed using a dual-band monopole antenna, an eigenmode feed network, and a sophisticated reactive decoupling network made up of a four-port 180° hybrid coupler. C-shaped and T-shaped slots, fed by microstrip lines, are used to produce dual band [51]. The mutual coupling of its constituent parts is reduced because of introducing the six sets of slits etched into its ground plane. In [52], two closely spaced chip antennas are used to create a dual-band MIMO antenna, and a pair of open-ended stubs is employed as a decoupling network at a higher frequency. In [53], the authors describe a dual-band MIMO antenna made up of two parallel folded branch monopoles with connected feed and an integrated isolation mechanism. Meandered monopoles are utilized to create dual-band antennas in [54], and a folded Y-shaped isolator is employed as a decoupling network between them. In [55], a dual-band MIMO antenna with two-port and four-port operations at the lower and upper bands, respectively, is demonstrated. Two $\lambda/4$ slots are etched at two resonant frequencies to improve separation. However, the abovementioned designs take up a lot of space and provide isolation of only around 20 dB at most. Thus, building a planar miniaturized dual-band MIMO antenna with good isolation between the ports at both operating bands is difficult.

The personal computer memory card found in laptop computers and other portable mobile devices are two examples of where MIMO antenna systems are put to use in WLAN mobile terminals. The antennas described in [56] are bulkier than those used in portable electronics. Positioning antennas in close proximity to one another result in mutual coupling, which decrease the antenna's performance. Many academics have looked into different methods to increase the isolation between the antenna elements in handheld devices. Using a combination of a rectangular slot ring and an inverted T-shaped slot, Meshram et al. [57] suggested a unique quad-band diversity antenna for LTE and Wi-Fi applications with excellent isolation. Lee et al. positioned a folded resonator atop the antenna to decrease the interaction between the antenna and the ground. To further increase the separation between the ports, a line is linked to the feeding strips of two P.I.F.As. To effectively reduce electromagnetic coupling between closely spaced antenna parts, researchers in [58] created single negative magnetic (M.N.G.) metamaterials. Min et al. [59] suggested a concept for wireless broadband MIMO and Personal Communication Systems (P.C.S) antennas that use a projected ground plane to mitigate the effects of mutual coupling.

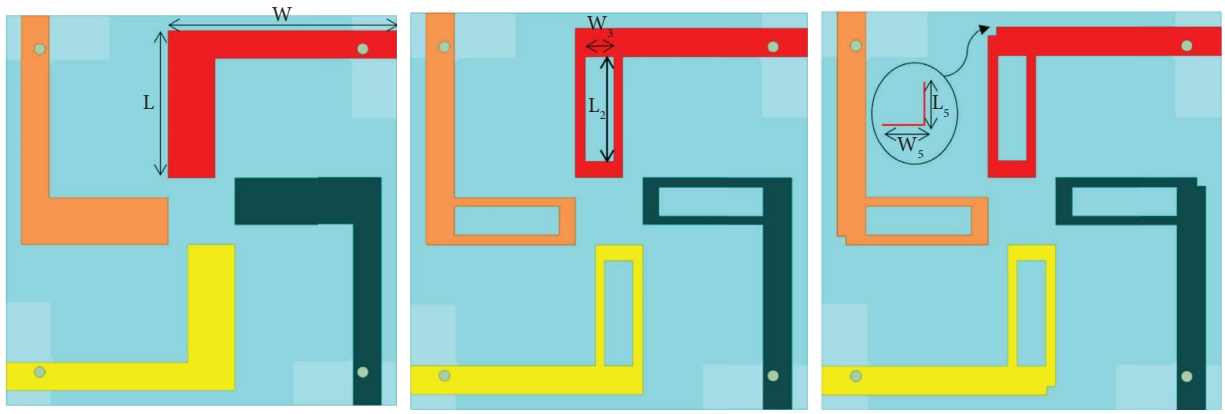

Figure 1: Design process of the proposed MIMO antenna.

Its ports are known to be particularly susceptible to mutual coupling. Thus researchers have looked into ways to mitigate this problem using parasitic elements [60] and decoupling approaches. All of the aforementioned methods in the literature [61] have fabrication issues, and some of them even decrease the antenna's reflection coefficient.

The research proposes a compact 2×2 MIMO antenna for WLAN band applications operating at 2.4 GHz. The proposed MIMO antenna consists of 4 identical L-shaped structures with a rectangular slot on the patch and introduces a small rectangular element as a ground plane.

3. Antenna Geometry

The proposed structure comprises four L-shaped monopole radiators and a small rectangular ground plane shown in Figure 1. The structure consists of 3 layers with ground and patch made up of copper material with a thickness of 0.1 mm, and a flame retardant (FR-4) substrate with material values ($\varepsilon_r = 4.4$ and $\tan\delta = 0.02$) is placed between the ground plane and patch elements with a thickness of $t = 1.96$ mm. The dimensions of the individual patch antenna chosen to be 16.251 mm × 25.733 mm are printed on the top of the FR4 substrate, and the individual ground plane with the size of 12 mm × 5.145 mm is printed on the bottom of the substrate. Each of the four elements is terminated by a 50 Ω coaxial connector located at the verge of the ground plane.

3.1. Antenna Design Process. Initially, the design starts with an L-shaped monopole radiator of size 26.61 mm × 17.12 mm and a ground plane of size 5.14 mm × 12 mm, and it is represented as Design I. The antenna operates at the frequency of 2.4 GHz with an S_{11} value of −23.4 dB, S_{21} value of −59.8 dB, S_{31} value of −53.1 dB, and S_{41} value of −51.6 dB. For the first design, isolation is high for opposite patches compared to the adjacent radiator. This is because the distance between radiators 1 and 2 is high when compared with adjacent radiators 13 and 14. Furthermore, in Design II, a rectangular slot is created at the center for all the radiating elements to improve the isolation between adjacent elements. As a result, it improves isolation for only one adjacent element with an S_{41} value of −54.53 dB. However, it still reduces the isolation for the opposite element with an S_{21} value of −51.3 dB and another adjacent element S_{31} value of −49.6 dB. Finally, in Design III, the truncated corner at one edge for all the radiating elements is created to improve the reflection coefficient and isolation parameter. As a result, design III improves the reflection coefficient S_{11} value of −28.8 dB, S_{21} value of −60.54 dB, S_{31} value of −66.3 dB, and S_{41} value of −58.4 dB. An isolation improvement for the proposed design is represented in Figure 1. The simulated scattering parameters for Designs I, II, and III are shown in Figure 2.

From Figure 2, it is observed that the simulated −10 dB impedance bandwidth lies between 2.31 GHz and 2.50 GHz with 2.4 GHz as the center frequency, whereas the mutual coupling among the various elements, denoted by $|S_{21}|$, $|S_{31}|$, and $|S_{41}|$, are found to be less than −58 dB in this entire band.

The proposed MIMO antenna with notations is mentioned in Figure 3, and their optimized values are given in Table 1.

4. Equivalent Circuit Model

The lumped-element (R.L.C.) model of the proposed MIMO antenna extracted using the advanced design system (A.D.S.) tool is shown in Figure 4. The mutual coupling between any two elements is denoted by a series inductor-capacitor (L.C.) circuit. The R, L, and C values are given in Table 2.

5. Results

Figure 5 shows the manufactured prototype of the proposed MIMO antenna with the measurement setup.

5.1. S-Parameters. Figure 6 shows the measured S-parameter values of the proposed antenna. The proposed antenna is designed at 2.4 GHz, but the dip frequency occurs at 2.24 GHz for the fabricated antenna. This is because the dielectric thickness used in the simulated design was 1.96 mm, and the MIMO antenna is fabricated on an FR-4 substrate with a thickness of 1.6 mm. There is a slight

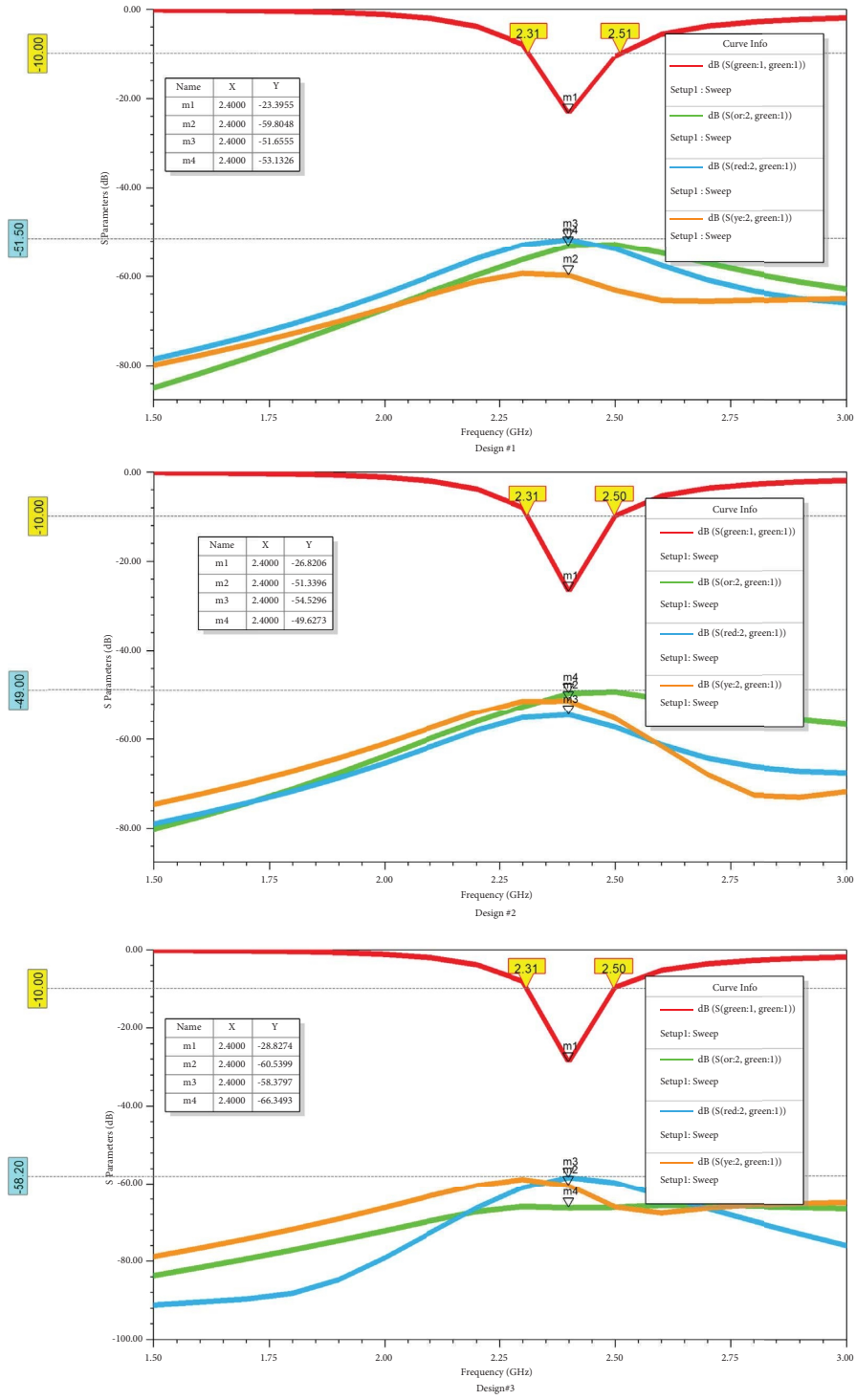

Figure 2: Simulated S parameters of design I, II, and III.

deviation in return loss parameters because of soldering effects in the S.M.A. connectors.

To visualize the mutual coupling effect between antenna elements, the surface current distribution of the MIMO antennas at 2.4 GHz is depicted in Figure 7. Even if the antennas are highly close to each other and if one antenna is excited, that radiated antenna will not interfere with the remaining antennas.

Exploiting the symmetry condition, an excitation signal is given at port 1. The remaining three ports are terminated with matched loads to measure antenna parameters like the radiation pattern, bandwidth, and peak gain. The distance between the ports is vital when determining how far the antenna elements are separated. Generally, when the antenna components are separated widely, there is a high isolation level. The proposed antenna shows high isolation

Table 1: The values of the proposed MIMO antenna.

Parameters	Values (mm)
L_1	16.25
L_2	12
L_3	3
L_4	28.35
W_1	25.73
W_2	3
W_3	5.41
W_4	2
G_1	12
G_2	5.14
D	7
L_{sub}	45.5
W_{sub}	45.5
L_5, W_5	0.87

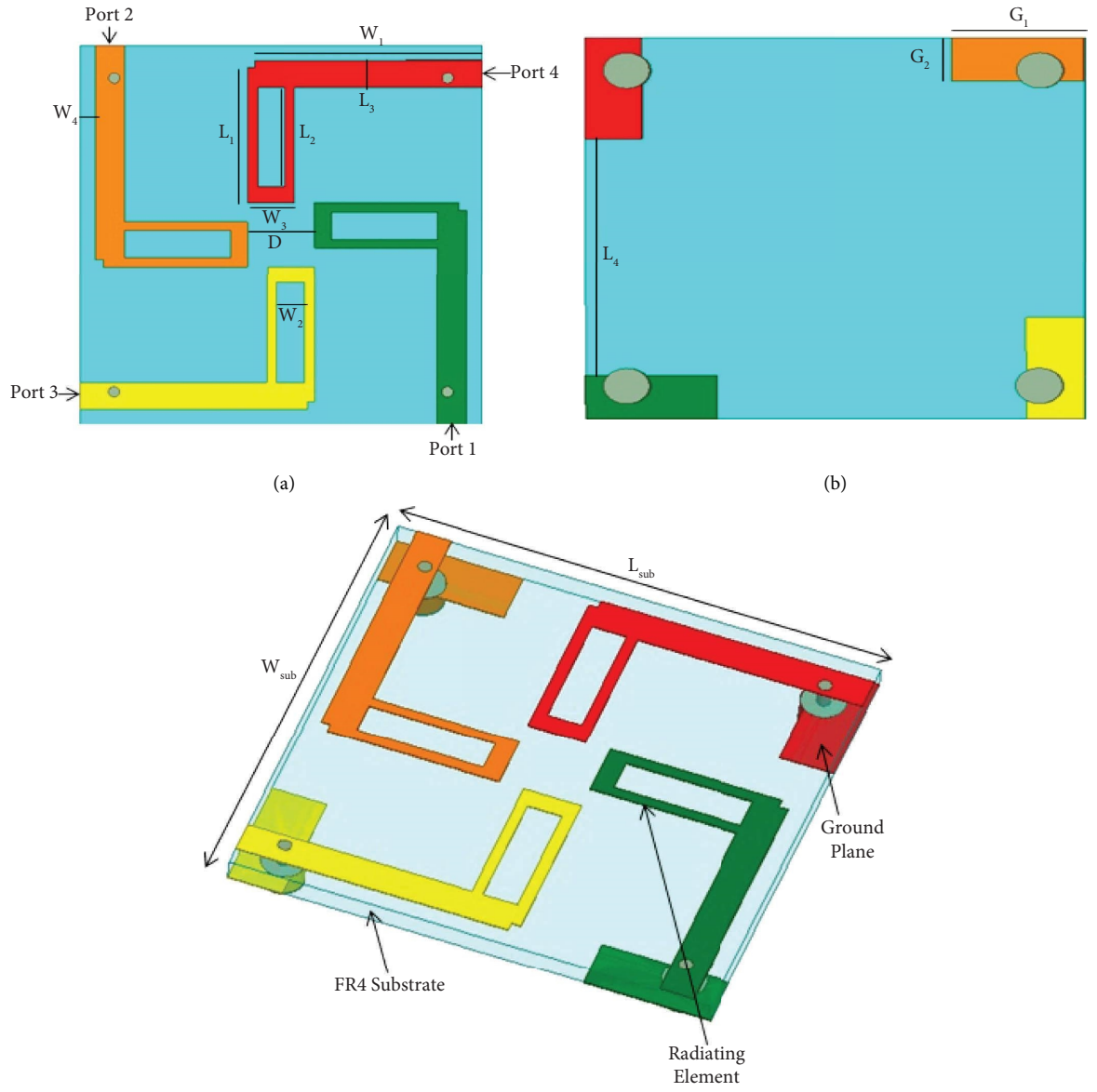

Figure 3: Proposed MIMO antenna structure. (a) Top view. (b) Bottom view. (c) 3D view.

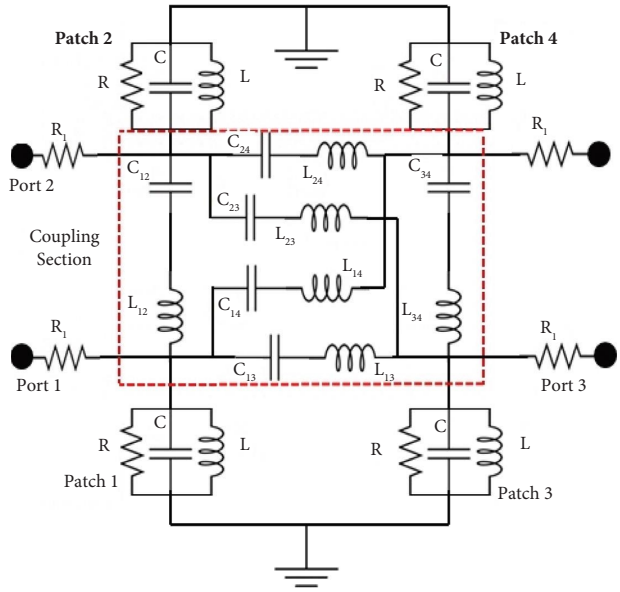

Figure 4: The equivalent R.L.C. circuit model of the proposed MIMO antenna.

Table 2: R.L.C. values of the equivalent circuit design.

Components	Values
R	16 Ω
L	18 nH
C	10.431 pF
R_1	1 Ω
L_{12}	2.53 nH
C_{12}	1.298 pF
C_{24}	9.66 pF
C_{23}	2.34 pF
L_{24}	19.176 nH
L_{14}	3.762 nH
L_{13}	13 nH
C_{13}	10.9 pF
L_{34}	26 nH
C_{34}	9.23 pF
C_{14}	2.33 pF
L_{23}	2.365 nH

between closely spaced antenna elements, and no mutual coupling happened between the multiple antennas, as shown in Figure 7.

5.2. Radiation Pattern. The simulated radiation patterns are plotted for only one port (port1) for $\phi = 0^\circ$ and $\phi = 90^\circ$ planes, while all the remaining ports are symmetrical in the MIMO antenna design. Figure 8 shows that the main beam directs maximum in the direction of 0° in both the planes (E-plane and H-plane).

The simulated radiation efficiency and gain versus frequency are plotted in Figure 9. From the figure, the peak gain of 2.8 dBi is obtained, and radiation efficiency is greater than 80% for the 2.4 GHz WLAN band.

The E.C.C. is a vital parameter to show the amount of correlation formed between interelement spacings. Here, the E.C.C. is calculated based on the scattering-parameter values [10, 37]. The calculated E.C.C. between the interelemental spacing for the MIMO antenna is shown in Figure 10.

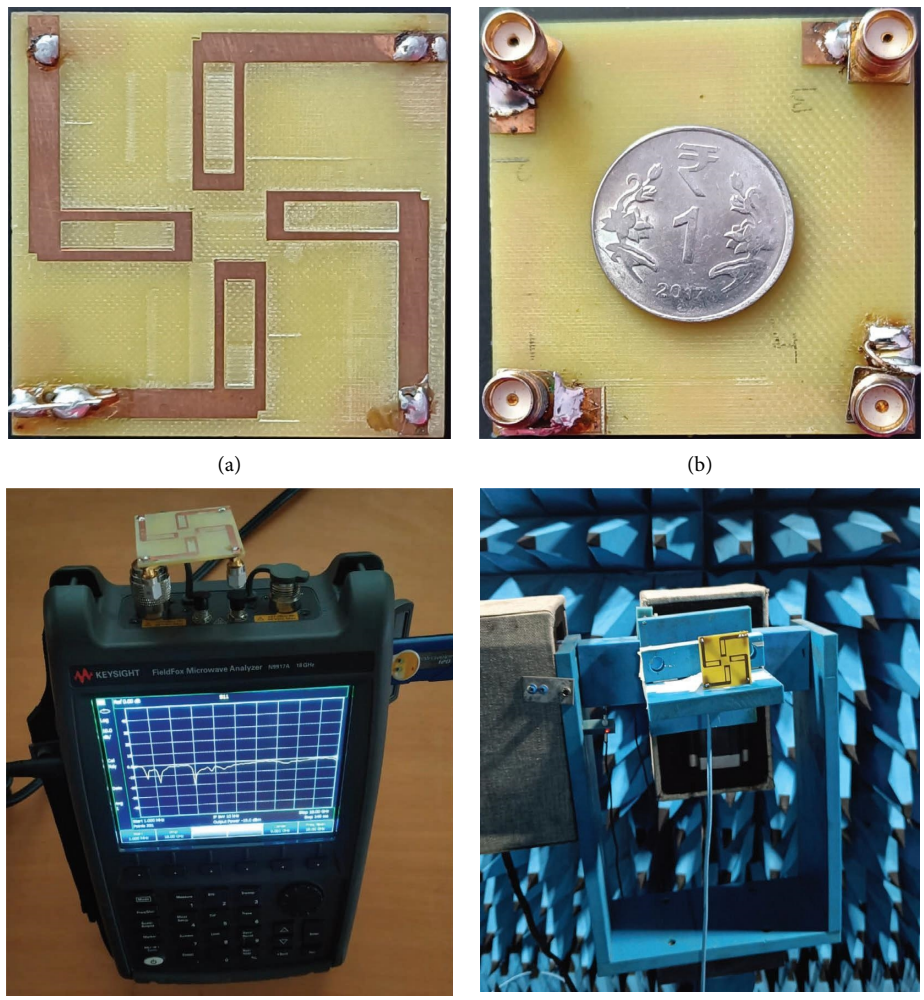

(a) (b)

(c) (d)

Figure 5: Photo of fabricated MIMO antenna. (a) Top view. (b) Rear view. (c) Antenna measurement setup using microwave analyzer N9917A. (d) Anechoic chamber testing.

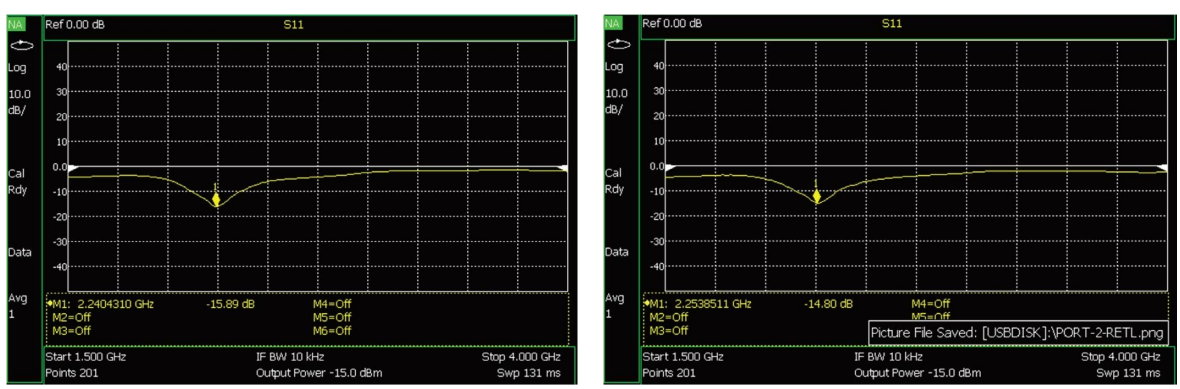

(a) (b)

Figure 6: Continued.

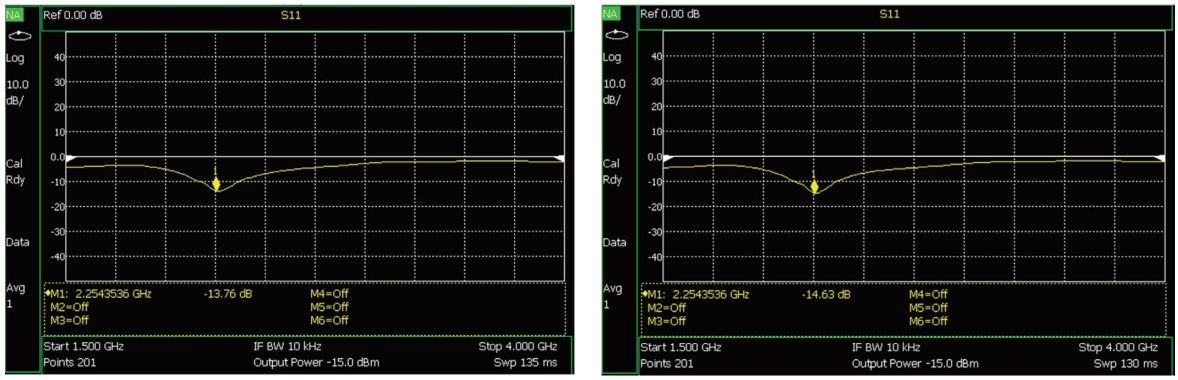

(c) (d)

Figure 6: Measured S-parameters of the proposed antenna. (a) Port 1. (b) Port 2. (c) Port 3. (d) Port 4.

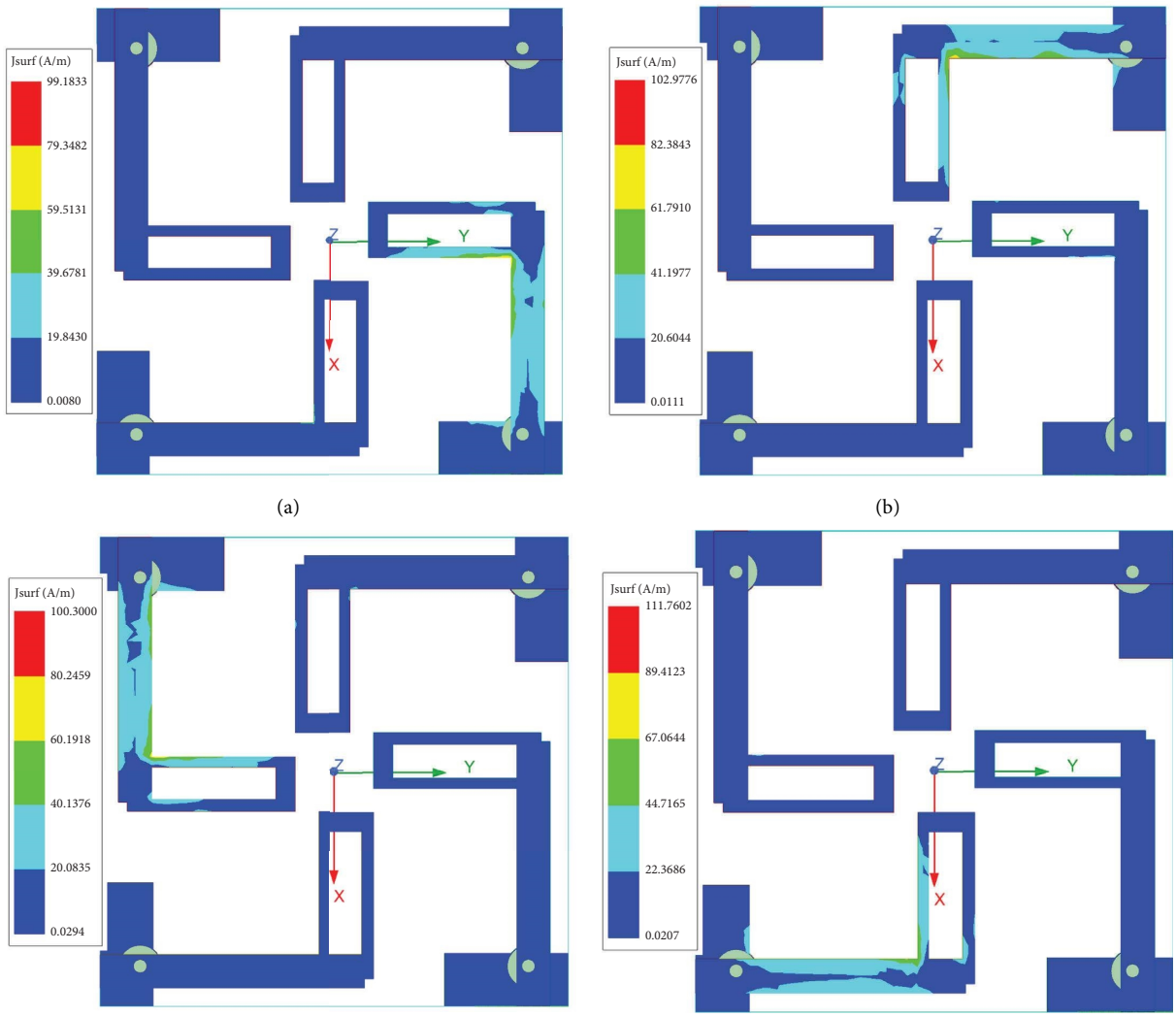

(a) (b)

(c) (d)

Figure 7: The current distribution of the proposed MIMO antenna at 2.4 GHz.

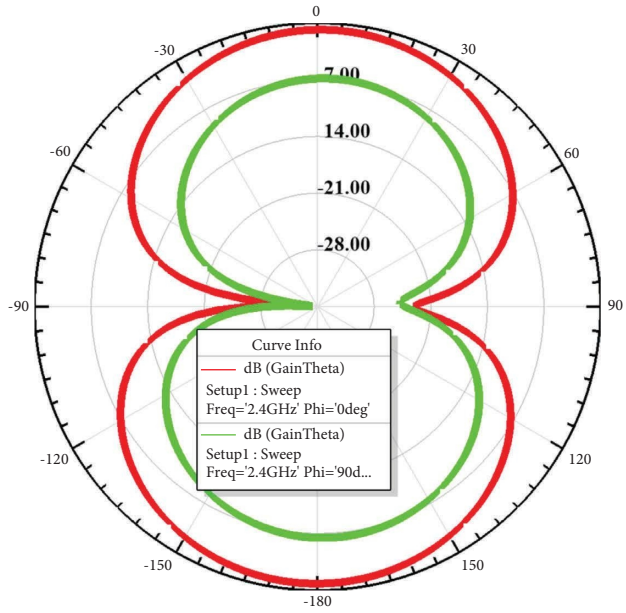

Figure 8: Simulated radiation patterns of the proposed antenna at 2.4 GHz.

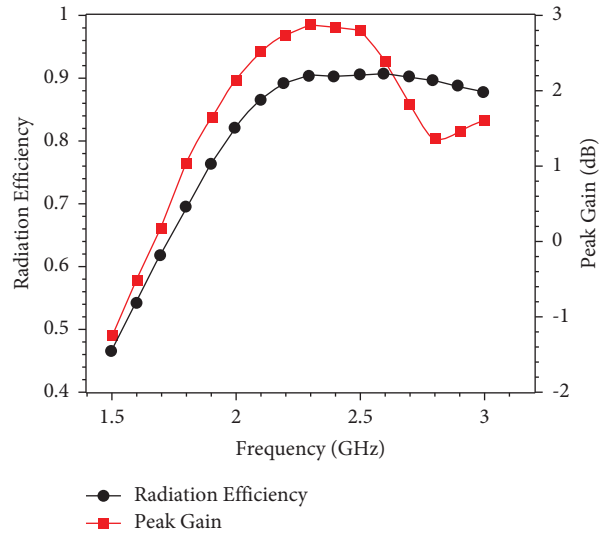

Figure 9: Radiation efficiency and gain of the proposed antenna.

The diversity gain is calculated based on the correlation coefficient values [23]. Any diversity scheme which improves the signal-to-interference ratio is referred to as diversity advantage. Since the antenna has a higher range gain value, it achieves greater separation and vice versa. Figure 10 shows a graphical view of the current MIMO antenna's diversity gain (D.G.). A well-defined comparison table of related works has been included to claim novelty for the proposed MIMO antenna. By the literature survey of MIMO antennas specified in Table 3, it witnesses well that the proposed MIMO has attained an improved isolation in contrast to antenna [8, 13, 21, 26, 38], low E.C.C compared to references [13, 16, 21, 29, 32], better radiation efficiency compared to references [8, 10, 16, 20, 26, 27], improved gain compared to referenes [7, 8, 10, 13, 27, 29], and smaller in size compared to references [7, 8, 10, 16, 20, 23, 27, 29, 32].

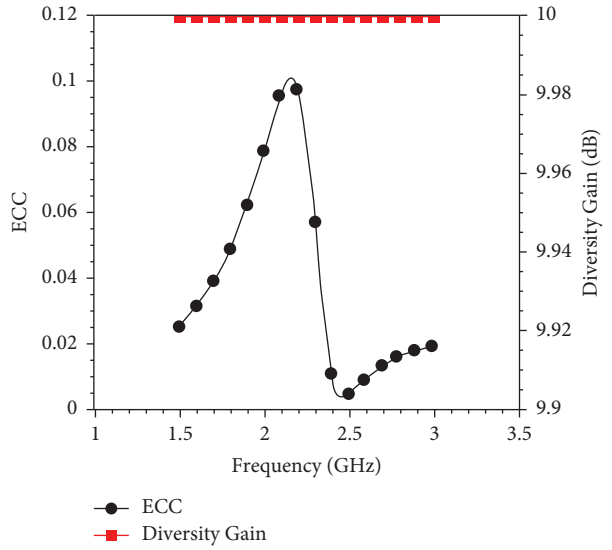

Figure 10: Diversity gain and the envelope correlation coefficient.

Table 3: Comparison of the proposed antenna with an existing published antenna.

References	Dimensions (mm^3)/material	Isolation levels (dB)	Gain (dBi)	Radiation efficiencies	E.C.C	D.G (dB)	No. of ports	Applications
[7]	$60.2 \times 60.2 \times 1.6$/FR-4	≥−25 dB at 2.45 GHz	2.2	81%	≤0.1	9.94	4	WLAN
[8]	$80 \times 80 \times 0.76$/Rogers 4350B	>10 at 2.4–2.8	>1.7	>67	<0.1	NG	8	WLAN
[10]	$100 \times 50 \times 0.8$/FR-4	≥−18 dB at 2.4~2.5 GHz	0.8	29%	≤0.3	9.53	4	I.S.M
[13]	$30 \times 65 \times 1$/FR-4	≥−15 dB at 2.4~2.5 GHz	2.1	81%	≤0.006	9.8	2	WLAN USB dongle
[16]	$90 \times 50 \times 0.8$/FR-4	≥−47 dB at 2.3~2.4 GHz	1.99~2.78	48.43~73.1%	≤0.0056~0.110	9.42~9.97	4	WiMax
[20]	$95 \times 95 \times 2.284$/Rogers RO4350 B	≥−25 dB at 2.395~2.42 GHz	5.12	56.57%	NG	NG/NG	4	ISM
[21]	$18.5 \times 18.5 \times 1.27$/ Rogers 6010LM	−15.99 at 2.4–2.48	−15.18	NG	0.0025	NG	4	Implantable
[22]	$20.5 \times 20.5 \times 1.6$/FR4	−32 at 2.45 GHz	2.6	55.44%	0.0081	NG	4	NG
[23]	$119 \times 119 \times 22.5$/Rogers RO4003, RO4450 B	≥−42 dB at 2.395–2.45 GHz	NG	NG/NG	<0.02	9.89	4	ISM
[26]	$112 \times 55 \times 1.6$/FR-4	≥−15 dB at 2.4 ~2.48 GHz	NG	66~75%	0.23~0.13	9.73~9.99	2	I.S.M
[27]	$72.4 \times 20 \times 0.8$/Rogers RO4350 B	≥−27.6 dB at 2.18 ~2.65 GHz	1.39	66~70.5%	0.08~0.09	9.96~9.95	2	I.S.M
[29]	$80 \times 80 \times 01.6$/FR-4 substrate	~20 dB at 2.5 GHz	NG	NG	0.054	9.68	2	LTE
[32]	$140 \times 120 \times 1.5$/FR4	−20 at 2.4–2.4835	NG	NG	<0.1	NG	4	WLAN
[38]	$34 \times 18 \times 1.6$/FR4	−15 at 2.45 GHz	1.26	76	0.12	NG	4	LTE 2300 and I.S.M
Proposed antenna	$45.5 \times 45.5 \times 1.96$/FR4	−58.37 at 2.4 GHz	2.84	90	0.0054	10	4	ISM

Bold indicates proposed antenna's parametrical values.

6. Conclusion

A compact L-shaped monopole radiator with a rectangular slot at the center of the patch and truncated corners at one edge is designed and validated. A comparison is made between the existing antenna and the proposed one's performance. Comparisons with similar MIMO antennas shown in Table 3 have reported that the proposed one is

small in size and offers excellent isolation without requiring a decoupling structure. In terms of expected crossover, the diversity performance is 0.0054. The MIMO antenna has high port-to-port isolation, low E.C.C., and high D.G. obtained within a compact volume of 45.5 mm × 45.5 mm × 1.96 mm. Based on these characteristics, it seems to be a good fit for WLAN uses involving Wi-Fi, I.S.M., and Bluetooth.

Data Availability

No data were used to support this study. Simulator tools are used to get the results, and VNA and chamber are used to verify the results.

Conflicts of Interest

The authors declare that they have no conflicts of interest.

References

[1] N. P. Kulkarni, N. Bhaskarrao Bahadure, P. D. Patil, and J. S. Kulkarni, "FlexibleInterconnected 4-port MIMO antenna for sub-6 GHz 5G and X band applications," *AEU-International Journal of Electronics and Communications*, vol. 152, Article ID 154243, 2022.

[2] J. Kulkarni, C. Y. D. Sim, A. Desai et al., "A compact four-port ground-coupled CPWG-fed MIMO antenna for wireless applications," *Arabian Journal for Science and Engineering*, vol. 47, no. 11, pp. 14087–14103, 2022.

[3] E. Wang, H. Shi, Y. Sun, C. Politis, L. Lan, and X. Chen, "Computer-aided porous implant design for craniomaxillofacial defect restoration," *The international journal of medical robotics + computer assisted surgery: MRCAS*, vol. 16, no. 5, pp. 1–10, 2020.

[4] J. Kulkarni, A. Desai, and C. Y. D. Sim, "Wideband Four-Port MIMO antenna array with high isolation for future wireless systems," *AEU - International Journal of Electronics and Communications*, vol. 128, Article ID 153507, 2021.

[5] A. W. Mohammad Saadh, K. Ashwath, P. Ramaswamy, T. Ali, and J. Anguera, "A uniquely shaped MIMO antenna on FR4 material to enhance isolation and bandwidth for wireless applications," *AEU - International Journal of Electronics and Communications*, vol. 123, Article ID 153316, 2020.

[6] M. S. Sadiq, C. Ruan, H. Nawaz, M. A. B. Abbasi, and S. Nikolaou, "Mutual coupling reduction between finite spaced planar antenna elements using modified ground structure," *Electronics*, vol. 10, p. 19, 2020.

[7] K. Wei, J. Li, L. Wang, Z. Xing, and R. Xu, "S-shaped periodic defected ground structures to reduce microstrip antenna array mutual coupling," *Electronics Letters*, vol. 52, no. 15, pp. 1288–1290, 2016.

[8] X. Hua, D. Wu, S. W. Cheung, and Q. L. Li, "A planar 8-port MIMO antenna for 2.4-GHz WLAN applications," in *Proceedings of the 2017 IEEE International Symposium on Antennas and Propagation & USNC/URSI National Radio Science Meeting*, pp. 1653-1654, San Diego, CA, USA, July 2017.

[9] A. K. Sohi and A. U. W. B. Kaur, "UWB aperture coupled circular fractal MIMO antenna with a complementary rectangular spiral defected ground structure (DGS) for 4G/WLAN/radar/satellite/international space station (ISS) communication systems," *Journal of Electromagnetic Waves and Applications*, vol. 34, no. 17, pp. 2317–2338, 2020.

[10] M. S. Sharawi, M. U. Khan, A. B. Numan, and D. N. Aloi, "A CSRR loaded MIMO antenna system for I.S.M. band operation," *IEEE Transactions on Antennas and Propagation*, vol. 61, no. 8, pp. 4265–4274, 2013.

[11] A. Ramachandran, S. Valiyaveettil Pushpakaran, M. Pezholil, and V. Kesavath, "A four-port MIMO antenna using concentric square-ring patches loaded with C.S.R.R. For high isolation," *IEEE Antennas and Wireless Propagation Letters*, vol. 15, no. c, pp. 1196–1199, 2016.

[12] L. Malviya, M. V. Kartikeyan, and R. K. Panigrahi, "Multistandard, multi-band planar multiple input multiple output antenna with diversity effects for wireless applications," *International Journal of RF and Microwave Computer-Aided Engineering*, vol. 29, no. 2, pp. e21551–e21558, 2019.

[13] S. W. Su, C. T. Lee, and F. S. Chang, "Printed MIMO-antenna system using neutralization-line technique for wireless USB-dongle applications," *IEEE Transactions on Antennas and Propagation*, vol. 60, no. 2, pp. 456–463, 2012.

[14] R. Liu, X. An, H. Zheng, M. Wang, Z. Gao, and E. Li, "Neutralization line decoupling tri-band multiple-input multiple-output antenna design," *IEEE Access*, vol. 8, pp. 27018–27026, 2020.

[15] R. N. Tiwari, P. Singh, B. K. Kanaujia, and K. Srivastava, "Neutralization technique based two and four port high isolation MIMO antennas for U.W.B. communication," *AEU - International Journal of Electronics and Communications*, vol. 110, Article ID 152828, 2019.

[16] J. H. Lim, Z. J. Jin, C. W. Song, and T. Y. Yun, "Simultaneous frequency and isolation reconfigurable MIMO PIFA using P.I.N. diodes," *IEEE Transactions on Antennas and Propagation*, vol. 60, no. 12, pp. 5939–5946, 2012.

[17] S. Soltani, P. Lotfi, and R. D. Murch, "A port and frequency reconfigurable MIMO slot antenna for WLAN applications," *IEEE Transactions on Antennas and Propagation*, vol. 64, no. 4, pp. 1209–1217, 2016.

[18] X. Zhao and S. Riaz, "A dual-band frequency reconfigurable MIMO patch-slot antenna based on reconfigurable microstrip feedline," *IEEE Access*, vol. 6, no. c, pp. 41450–41457, 2018.

[19] M. Alibakhshikenari, B. S. Virdee, P. Shukla et al., "Isolation enhancement of densely packed array antennas with periodic MTM-photonic bandgap for SAR and MIMO systems," *IET Microwaves, Antennas & Propagation*, vol. 14, no. 3, pp. 183–188, 2020.

[20] Y. Fan, J. Huang, T. Chang, and X. Liu, "A miniaturized four-element MIMO antenna with E.B.G. for implantable medical devices," *IEEE Journal of Electromagnetics, RF and Microwaves in Medicine and Biology*, vol. 2, no. 4, pp. 226–233, 2018.

[21] S. Ghosh, T. N. Tran, and T. Le-Ngoc, "Dual-layer EBG-based miniaturized multi-element antenna for MIMO systems," *IEEE Transactions on Antennas and Propagation*, vol. 62, no. 8, pp. 3985–3997, 2014.

[22] M. Alibakhshikenari, M. Khalily, B. S. Virdee, C. H. See, R. A. Abd-Alhameed, and E. Limiti, "Mutual coupling suppression between two closely placed microstrip patches using EM-bandgap metamaterial fractal loading," *IEEE Access*, vol. 7, no. c, pp. 23606–23614, 2019.

[23] G. Zhai, Z. N. Chen, and X. Qing, "Enhanced isolation of a closely spaced four-element MIMO antenna system using metamaterial mushroom," *IEEE Transactions on Antennas and Propagation*, vol. 63, no. 8, pp. 3362–3370, 2015.

[24] M. Alibakhshikenari, M. Khalily, B. S. Virdee, C. H. See, R. A. Abd-Alhameed, and E. Limiti, "Mutual-coupling isolation using embedded metamaterial E.M. bandgap

decoupling slab for densely packed array antennas," *IEEE Access*, vol. 7, pp. 51827–51840, 2019.

[25] M. Alibakhshikenari, B. S. Virdee, C. H. See et al., "Study on isolation improvement between closely-packed patch antenna arrays based on fractal metamaterial electromagnetic bandgap structures," *IET Microwaves, Antennas & Propagation*, vol. 12, no. 14, pp. 2241–2247, 2018.

[26] M. Li, L. Jiang, and K. L. Yeung, "Novel and efficient parasitic decoupling network for closely coupled antennas," *IEEE Transactions on Antennas and Propagation*, vol. 67, no. 6, pp. 3574–3585, 2019.

[27] K. Qian, L. Zhao, and K. L. Wu, "An LTCC coupled resonator decoupling network for two antennas," *IEEE Transactions on Microwave Theory and Techniques*, vol. 63, no. 10, pp. 3199–3207, 2015.

[28] D. Wu, S. W. Cheung, Q. L. Li, and T. I. Yuk, "Decoupling using diamond-shaped patterned ground resonator for small MIMO antennas," *IET Microwaves, Antennas & Propagation*, vol. 11, no. 2, pp. 177–183, 2017.

[29] J. Nasir, M. H. Jamaluddin, M. Khalily, M. R. Kamarudin, and I. Ullah, "Design of an MIMO dielectric resonator antenna for 4G applications," *Wireless Personal Communications*, vol. 88, no. 3, pp. 525–536, 2016.

[30] G. Das, A. Sharma, and R. K. Gangwar, "Dual port aperture coupled MIMO cylindrical dielectric resonator antenna with high isolation for WiMAX application," *International Journal of RF and Microwave Computer-Aided Engineering*, vol. 27, no. 7, pp. e21107–e21110, 2017.

[31] S. S. Singhwal, B. K. Kanaujia, A. Singh, and J. Kishor, "Dual-port MIMO dielectric resonator antenna for WLAN applications," *International Journal of RF and Microwave Computer-Aided Engineering*, vol. 30, no. 4, pp. 1–11, 2020.

[32] S. Palanisamy, B. Thangaraju, O. I. Khalaf, Y. Alotaibi, S. Alghamdi, and F. Alassery, "A novel approach of design and analysis of a hexagonal fractal antenna array (HFAA) for next-generation wireless communication," *Energies*, vol. 14, no. 19, p. 6204, 2021.

[33] M. Alibakhshikenari, B. S. Virdee, P. Shukla et al., "Antenna mutual coupling suppression over wideband using embedded periphery slot for antenna arrays," *Electronics*, vol. 7, no. 9, p. 198, 2018.

[34] T. Addepalli and V. R. Anitha, "Compact two-port mimo antenna with high isolation using parasitic reflectors for uwb, x and ku band applications," *Progress in Electromagnetics Research C*, vol. 102, pp. 63–77, 2020.

[35] M. A. Ul Haq and S. Koziel, "Ground plane alterations for design of high-isolation compact wideband MIMO antenna," *IEEE Access*, vol. 6, no. c, pp. 48978–48983, 2018.

[36] T. Prabhu and S. C. Pandian, "Design and development of planar antenna array for mimo application," *Wireless Networks*, vol. 27, no. 2, pp. 939–946, 2021.

[37] S. Kumar, R. Kumar, R. Kumar Vishwakarma, and K. Srivastava, "An improved compact MIMO antenna for wireless applications with band-notched characteristics," *AEU - International Journal of Electronics and Communications*, vol. 90, pp. 20–29, 2018.

[38] M. Alibakhshikenari, F. Babaeian, B. S. Virdee et al., "A comprehensive survey on "Various decoupling mechanisms with focus on metamaterial and metasurface principles applicable to S.A.R. and MIMO antenna systems," *IEEE Access*, vol. 8, pp. 192965–193004, 2020.

[39] D. S, S. Palanisamy, F. Hajjej, O. I. Khalaf, G. M. Abdulsahib, and R. S, "Discrete fourier transform with denoise model based least square wiener channel estimator for channel estimation in MIMO-OFDM," *Entropy*, vol. 24, no. 11, p. 1601, 2022.

[40] P. Satheesh Kumar and M. Jeevitha, "Diagnosing COVID-19 virus in the cardiovascular system using ANN," in *Artificial Intelligence for COVID-19. Studies in Systems, Decision and Control*, D. Oliva, S. A. Hassan, and A. Mohamed, Eds., vol. 358, Cham, Switzerland, Springer, 2021.

[41] M. M. Hasan, M. T. Islam, M. Samsuzzaman et al., "Gain and isolation enhancement of a wideband MIMO antenna using metasurface for 5G sub-6 GHz communication systems," *Scientific Reports*, vol. 12, p. 9433, 2022.

[42] M. Alibakhshikenari, B. S. Virdee, C. H. See, R. A. Abd-Alhameed, F. Falcone, and E. Limiti, "Surface wave reduction in antenna arrays using metasurface inclusion for MIMO and S.A.R. systems," *Radio Science*, vol. 54, no. 11, pp. 1067–1075, 2019.

[43] M. Alibakhshikenari, B. S. Virdee, P. Shukla et al., "Interaction between closely packed array antenna elements using metasurface for applications such as MIMO systems and synthetic aperture radars," *Radio Science*, vol. 53, no. 11, pp. 1368–1381, 2018.

[44] M. Alibakhshikenari, B. S. Virdee, P. Shukla et al., "Metasurface wall suppression of mutual coupling between microstrip patch antenna arrays for THz-band applications," *Progress In Electromagnetics Research Letters*, vol. 75, pp. 105–111, 2018.

[45] R. Karimian, H. Oraizi, S. Fakhte, and M. Farahani, "Novel F-shaped quad-band printed slot antenna for WLAN and WiMAX MIMO systems," *IEEE Antennas and Wireless Propagation Letters*, vol. 12, no. c, pp. 405–408, 2013.

[46] S. Palanisamy, B. Thangaraju, O. I. Khalaf, Y. Alotaibi, and S. Alghamdi, "Design and synthesis of multi-mode bandpass filter for wireless applications," *Electronics*, vol. 10, no. 22, p. 2853, 2021.

[47] T. Nivethitha, S. K. Palanisamy, K. MohanaPrakash, and K. Jeevitha, "Comparative study of ANN and fuzzy classifier for forecasting electrical activity of heart to diagnose Covid-19," *Materials Today: Proceedings*, vol. 45, pp. 2293–2305, 2021.

[48] A. Kandasamy, S. Rengarasu, P. Kitti Burri et al., "Defected circular-cross stub copper metal printed pentaband antenna," *Advances in Materials Science and Engineering*, vol. 2022, Article ID 6009092, 10 pages, 2022.

[49] P. Satheesh Kumar and J. Manikandan, "Diagnosing COVID-19 virus in the cardiovascular system using ANN," in *Artificial Intelligence for COVID-19, Studies in Systems, Decision and Control*, D. Oliva, S. A. Hassan, and A. Mohamed, Eds., vol. 358, Springer, Cham, Switzerland, 2021.

[50] P. J. C. Sam, U. Surendar, U. M. Ekpe, M. Saravanan, and P. Satheesh Kumar, "A low-profile compact EBG integrated circular monopole antenna for wearable medical application," in *Smart Antennas. EAI/Springer Innovations in Communication and Computing*, P. K. Malik, J. Lu, B. T. P. Madhav, G. Kalkhambkar, and S. Amit, Eds., Springer, Cham, Switzerland, 2022.

[51] T. Prabhu, E. Suganya, J. Ajayan, and P. S. Kumar, "An intensive study of dual patch antennas with improved isolation for 5G mobile communication systems," *Future Trends in 5G and 6G*, CRC Press, Boca Raton, FL, USA, 205-217.

[52] P. Satheesh Kumar and S. Valarmathy, "Development of a novel algorithm for S.V.M.B.D.T. fingerprint classifier based on clustering approach," in *Proceedings of the IEEE-International Conference on Advances In Engineering, Science*

And Management (I.C.A.E.S.M. -2012), pp. 256–261, Nagapattinam, India, October 2012.

[53] S. Kumar and T. Balakumaran, "Modeling and simulation of dual layered U-slot multiband microstrip patch antenna for wireless applications," *Nanoscale Reports*, vol. 4, no. 1, pp. 15–18, 2021.

[54] P. S. Kumar, P. Chitra, and S. Sneha, "Design of improved quadruple-mode bandpass filter using cavity resonator for 5G mid-band applications," *Future Trends in 5G and 6G: Challenges, Architecture, and Applications*, p. 219, CRC Press, Boca Raton, FL, USA, 2021.

[55] S. Palanisamy and B. Thangaraju, "Design and analysis of clover leaf-shaped fractal antenna integrated with stepped impedance resonator for wireless applications," *International Journal of Communication Systems*, vol. 35, no. 11, 2022.

[56] Y. K. Choukiker, S. K. Sharma, and S. K. Behera, "Hybrid fractal shape planar monopole antenna covering multiband wireless communications with MIMO implementation for handheld mobile devices," *IEEE Transactions on Antennas and Propagation*, vol. 62, no. 3, pp. 1483–1488, 2014.

[57] M. K. Meshram, R. K. Animeh, A. T. Pimpale, and N. K. Nikolova, "A novel quad-band diversity antenna for LTE and Wi-Fi applications with high isolation," *IEEE Transactions on Antennas and Propagation*, vol. 60, no. 9, pp. 4360–4371, 2012.

[58] X. Xue, R. Shanmugam, S. Palanisamy, O. I. Khalaf, D. Selvaraj, and G. M. Abdulsahib, "A hybrid cross layer with harris-hawk-optimization-based efficient routing for wireless sensor networks," *Symmetry*, vol. 15, no. 2, p. 438, 2023.

[59] K. S. Min, M. S. Kim, C. K. Park, and M. Vu, "Design for P.C.S. antenna based on WiBro-MIMO," *Progress In Electromagnetics Research Letters*, vol. 1, pp. 77–83, 2008.

[60] K. Suganyadevi, V. Nandhalal, S. Palanisamy, and S. Dhanasekaran, "Data security and safety services using modified timed efficient stream loss-tolerant authentication in diverse models of VANET," in *Proceedings of the 2022 International Conference on Edge Computing and Applications (ICECAA)*, pp. 417–422, Tamilnadu, India, October 2022.

[61] M. El Gharbi, R. Fernández-García, S. Ahyoud, and I. Gil, "A review of flexible wearable antenna sensors: design, fabrication methods, and applications," *Materials*, vol. 13, no. 17, p. 3781, 2020.